Available online at www.sciencedirect.com
SCIENCE DIRECT®
ELSEVIER
International Journal of Impact Engineering 32 (2005) 650–664
INTERNATIONAL JOURNAL OF IMPACT ENGINEERING
www.elsevier.com/locate/ijimpeng

Dynamic crushing of 2D cellular structures: A finite element study

Zhijun Zheng, Jilin Yu*, Jianrong Li

CAS Key Laboratory of Mechanical Behavior and Design of Materials, University of Science and Technology of China, Hefei, Anhui 230026, PR China

Received 6 September 2004; received in revised form 22 February 2005; accepted 20 May 2005
Available online 22 July 2005

Abstract

The dynamic crushing behavior of 2D cellular structures is studied by finite element method using ABAQUS/Explicit code. The influences of cell irregularity and impact velocity on the deformation mode and the plateau crush pressure are investigated. Two irregularity-generating methods are used. One is the disorder of nodal locations of a regular hexagonal honeycomb and the other is based on the 2D random Voronoi technique. The results show that the deformation in an irregular honeycomb is more complicated than that in a regular honeycomb due to its cell irregularity. At a low impact velocity, a Quasi-static mode with multiple random shear bands appears, while at a higher impact velocity, a Transitional mode is found, i.e., a mode with localized random shear bands and layerwise collapse bands. Finally, at a much higher impact velocity, a Dynamic mode appears with a narrow localized layerwise collapse band near the crushed end. The velocities for transition between modes are evaluated and expressed by empirical equations. Deformation anisotropy is found in the response of disordered honeycombs but it vanishes with the increase in the irregularity. Statistical results show that the relative energy absorption capacity of cellular materials can be improved by increasing their cell irregularity. This effect is obvious especially at an impact velocity near the mode transition velocity.

Keywords: Dynamic crushing; Cellular materials; Irregular honeycomb; Voronoi structure; Finite element analysis

*Corresponding author. Tel.: +86 551 360 3793; fax: +86 551 360 6459.
E-mail address: jlyu@ustc.edu.cn (J. Yu).

0734-743X/$ - see front matter © 2005 Elsevier Ltd. All rights reserved.
doi:10.1016/j.ijimpeng.2005.05.007

1. Introduction

Metallic honeycombs and foams are widely used as advanced structural components in many engineering applications due to their excellent mechanical properties and energy absorption capacity. Much work has shown that the mechanical properties of cellular materials are affected by the micro-structural parameters such as relative density, cell size and cell morphology. Experimental and theoretical studies on their mechanical behavior have focused on the elastic moduli and plastic collapse strength. In recent years, finite element analyses (FEA) have been carried out to investigate the influence of the micro-structural parameters of metallic honeycombs and foams on their crushing behavior.

Gibson and Ashby have systematically presented the in-plane and out-of-plane properties of honeycombs under static crushing in their literature review [1]. Since a cellular structure is an assembly of periodically or nearly periodically basic cells, Shi and Tong [2] derived the equivalent transverse shear modulus and in-plane modulus of honeycombs based on a two-scale method for the homogenization of periodic media. Wang et al. [3] generalized the rotation stiffness method to incorporate the elastic–plastic analysis of honeycomb cell walls. They employed a representative unit cell (RUC) with imperfections to numerically simulate the mechanical behaviors of elastic–plastic deformation, instability and collapse of single-type aluminum honeycombs under uniaxial compression. Papka and Kyriakides [4–8] carried out experiments and full-scale numerical simulations to study the in-plane uniaxial and biaxial crushing behavior of honeycombs. The biaxial crushing is helpful to understanding the associated deformation mechanisms, but it is quite complex to perform these experiments; they have been achieved by Papka and Kyriakides [7] who designed and built a custom biaxial crushing machine (BICRUMA). Recently, full-scale numerical simulations have attracted considerable research interest due to the localization of deformation. Considering geometric and material imperfections of aluminum honeycomb specimens used in engineering applications, Triantafyllidis and Schraad [9] studied the effects of imperfections on the quasi-static deformation and failure of double-type honeycombs under biaxial loading and found that their behavior was sensitive to the imperfections. Fortes and Ashby [10] analyzed the effect of non-uniformity on the in-plane Young's modulus of 2D foams with a distribution of the cell wall lengths and thicknesses. Chen et al. [11] studied systematically the influence of six types of morphological imperfection (waviness, non-uniform thickness of cell edges, cell-size variations, fractured cell walls, cell-wall misalignments, and missing cells) on the yielding of 2D cellular solids under biaxial loading. Using the finite element method, intact and damaged honeycombs [12], Voronoi honeycombs [13,14] and their extension exhibiting bimodal or multimodal cell size distributions [15] were employed to analyze the influence of the imperfection on the static crushing behavior.

The dynamic crushing behavior of honeycombs also attracted considerable research interest. Zhao and Gray [16] presented an experimental study on the in-plane and out-of-plane dynamic crushing behavior of honeycombs using a Split Hopkinson Pressure Bar (SHPB) apparatus. Hönig and Stronge [17,18] presented a finite element simulation to study the in-plane crushing of honeycombs. Ruan et al. [19] investigated the influences of the cell wall thickness and the impact velocity on the mode of localized deformation and the plateau crush pressure by means of finite element simulation using ABAQUS. They found that there are three types of deformation modes

in the x_1 direction and two types of deformation modes in the x_2 direction, which were summarized in a mode classification map.

Recently, Yu et al. [20] studied the quasi-static and dynamic crushing behavior of closed-cell aluminum foams, respectively, on an MTS810 testing system and an SHPB apparatus. Both the strain-rate effect and the cell-size effect on the crushing stress were found. The results reveal that the structural heterogeneity and irregularity have influences on the strain-rate sensitivity of cellular metals. So it is of great significance to study the influence of the micro-structural parameters on the impact crushing behavior of realistic honeycombs and foams.

In this paper two irregularity-generating methods are employed to create irregular honeycomb models. The in-plane dynamic behavior of these structures is then studied by finite element simulation using ABAQUS/Explicit code [21]. The influences of cell irregularity and impact velocity on the deformation mode and the plateau crush pressure are investigated.

2. Computational models

2.1. Irregularity-generating methods

Two irregularity-generating methods are employed. One is the disorder of nodal locations of a regular hexagonal honeycomb, and the other is based on the 2D random Voronoi technique.

2.1.1. Disorder of nodal locations of a regular hexagonal honeycomb

Each node of a regular hexagonal honeycomb is randomly disordered from its original position by

$$\begin{aligned} x_i &= x_{0i} + \Delta_i \cos\theta_i, \\ y_i &= y_{0i} + \Delta_i \sin\theta_i, \end{aligned} \tag{1}$$

as shown in Fig. 1a, where (x_{0i}, y_{0i}) are the coordinates of the ith node of the regular honeycomb, (x_i, y_i) are the corresponding coordinates after distortion, Δ_i is a random length $(0 \leqslant \Delta_i \leqslant \Delta)$, and θ_i a random angle $(0 \leqslant \theta_i \leqslant 2\pi)$.

In order to generate a disordered honeycomb with certain irregularity, Δ is restricted within a limit. The irregularity of the disordered honeycomb can be defined as

$$k_1 = \frac{\Delta}{l_0/2}, \tag{2}$$

where l_0 is the cell wall length of the regular honeycomb.

2.1.2. 2D random voronoi technique

N nuclei are generated in a square area A_0 by the principle that the distance between any two points is not less than a given distance δ. Then these nuclei are copied to the surrounding neighboring areas by translation. Use the set of these $9N$ nuclei to construct the Delaunay triangulation and even the Voronoi diagram. The condition satisfied by a Voronoi cell is that it contains all points that are closer to its data point than any other data point in the set. Finally, the part of the Voronoi diagram out of the square area A_0 is deleted to reserve a periodic Voronoi

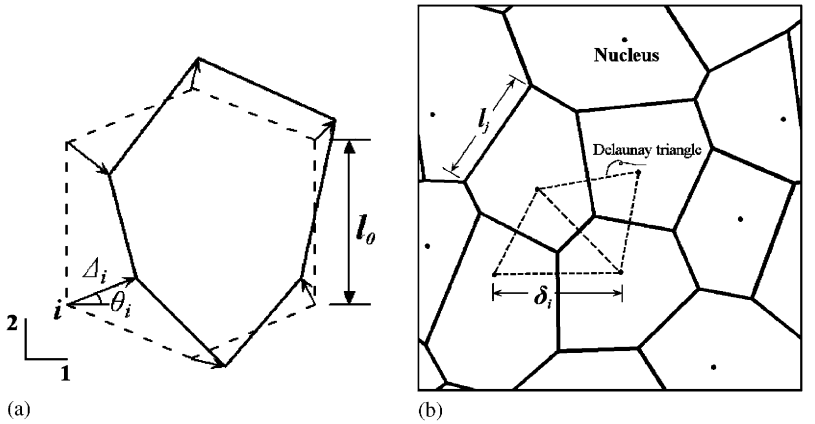

Fig. 1. Two irregularity-generating methods: (a) disorder of a regular hexagonal honeycomb, (b) 2D random Voronoi technique.

structure. The character of this 2D random Voronoi technique is hinted in Fig. 1b. For more details the reader is referred to Refs. [22,23].

To construct a regular hexagonal honeycomb with N cells in the square area A_0, the distance between any two adjacent nuclei is given by

$$\delta_0 = \sqrt{2A_0/\sqrt{3}N}. \tag{3}$$

For a 2D random Voronoi honeycomb with N cells in the square area A_0, the irregularity of the Voronoi honeycomb can be defined as

$$k_2 = 1 - \delta/\delta_0, \tag{4}$$

where δ is the minimum distance between any two nuclei [14,23].

2.2. Finite element models

In our finite element models, the cell wall material is taken to be elastic-perfectly plastic. Its Young's modulus, yield stress, Possion's ratio and mass density are assigned as 69 GPa, 76 MPa, 0.3 and 2.7×10^3 kg/m^3, respectively, the same as those used by Ruan et al [19]. The cell wall thickness is $h = 0.09$ mm for all cases. Each edge of the cell wall is modeled with about 6 shell elements of type S4R (a 4-node quadrilateral shell element with reduced integration) with 5 integration points.

Fig. 2a shows a regular hexagonal honeycomb (denoted here as Model A) with a cell wall length of $l_0 = 3$ mm.The size is 103.92 mm × 87 mm. It has 20 cells in the x_1 direction and 19 in the x_2 direction. Irregular honeycombs are created based on the disorder of nodal locations of this honeycomb. Two samples are shown in Figs. 2b and c, corresponding to an irregularity of 0.4 and 0.8, respectively. In these models, each edge of the cell wall is divided into 6 shell elements and each model consists of a total of 7140 shell elements.

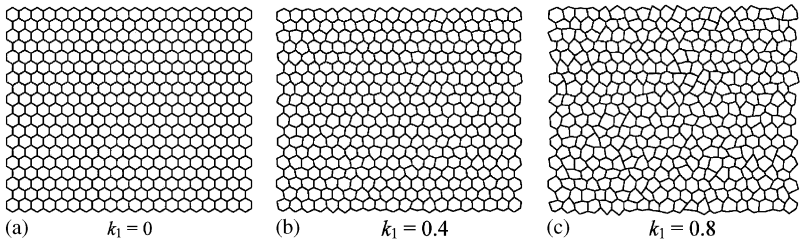

Fig. 2. Disordered honeycombs.

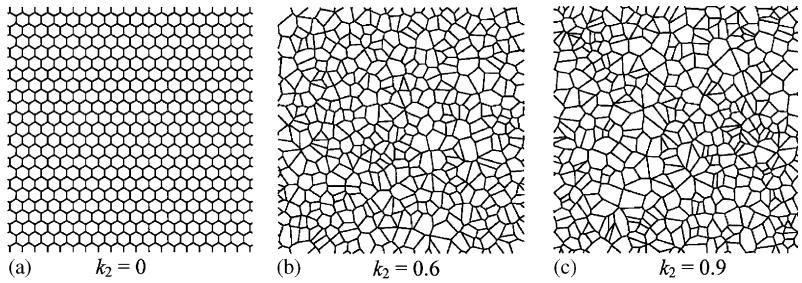

Fig. 3. Voronoi honeycombs.

Voronoi honeycomb samples are constructed in an area of $100\,mm \times 100\,mm$ with 400 nuclei. Two samples are shown in Figs. 3b and c, corresponding to an irregularity of 0.6 and 0.9, respectively; while a referential regular hexagonal honeycomb (denoted as Model B) is shown in Fig. 3a. Cell walls shorter than the thickness were eliminated and the associated cell corners merged to ensure the process of the FEA, similar as that used by Schaffner et al [24]. Each edge of the cell wall is divided into shell elements according to its length, with the mean element length of about 0.5 mm. Each model consists of about 7500 shell elements. It can be seen that the scatter of cell size increase with the increase of the irregularity. For a Voronoi honeycomb with an irregularity of 0.9, size of some cells may be two times larger or smaller than that of a regular honeycomb.

Each cell is defined as a single self-contact surface. Self-contact is also specified between the outside faces of a cell that may contact other cells during crushing. This self-contact definition is easy to carry out for disordered honeycombs. For Voronoi honeycombs, an outside layer is added to carry out this self-contact. Through a convergence study, the outside layer thickness is taken as 1/10 of the cell wall thickness. In the simulation, the honeycomb is sandwiched between two rigid platens and its contact edges can slip on both interfaces with slight friction. The friction coefficient is assumed as 0.02. When crushing in the x_1 direction, the top and bottom edges are free and the left platen is stationary, and the right platen moves leftward with a constant velocity. Similarly, when crushing in the x_2 direction, the left and right edges are free and the bottom platen is stationary, and the top platen moves downward with a constant velocity.

2.3. Computational aspects

2.3.1. Relative density

The relative density of a honeycomb is specified by

$$\rho = \rho^*/\rho_s = \frac{\sum h_i l_i}{L_1 L_2}, \tag{5}$$

where ρ^* is the density of honeycomb, ρ_s the density of honeycomb cell wall material, l_i the ith cell wall length and h_i the corresponding thickness, L_1 and L_2 are the width and height of the specimen, respectively. The cell wall thickness is identical, i.e., $h_i = h = 0.09$ mm for both disordered honeycombs and Voronoi honeycombs, except that of the outside layer of Voronoi honeycombs, as mentioned above. The statistical values of the relative density of disordered and Voronoi honeycombs are shown in Fig. 4a. It transpires that all these values are about 0.036.

2.3.2. Average number of edges per cell and its second moment

The morphological characteristics of irregular honeycombs are usually described by the average number of edges per cell μ and its second moment μ_2, which are defined by

$$\mu = \frac{1}{N_c}\sum_{i=1}^{N_c} n_i,$$

$$\mu_2 = \frac{1}{N_c}\sum_{i=1}^{N_c}(n_i - \mu)^2, \tag{6}$$

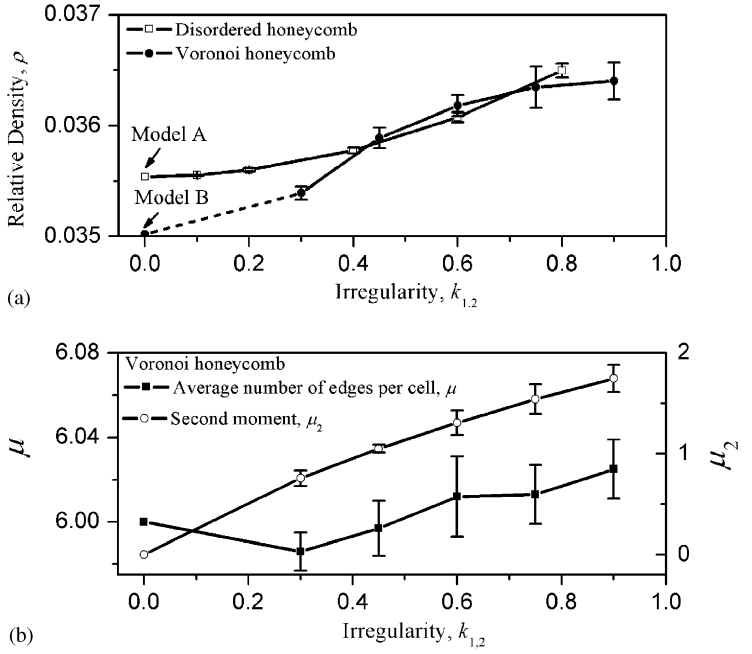

Fig. 4. The statistical values of (a) relative density, (b) average number of edges per cell and its second moment of irregular honeycombs, i.e., disordered honeycombs with 20 samples and Voronoi honeycombs with 10 samples.

where n_i is the number of edges of the ith cell and N_c the total number of cells. For any disordered honeycomb with an irregularity of $k_1 < 1$, the average number of edges per cell is 6 and its second moment is 0. For Voronoi honeycombs, the statistical results are shown in Fig. 4b.

3. Results

3.1. Deformation modes

3.1.1. Deformation modes of regular honeycombs

For regular honeycombs, Ruan et al. [19] have shown that the inertia effect plays an important role in dynamic crushing. When crushing in the x_1 direction, three types of deformation modes are observed. At a low impact velocity, localized deformation causes oblique "X"-shaped bands ("X" mode); at a high impact velocity, it produces transverse localized bands ("I" mode) oriented perpendicular to the loading direction and located adjacent to the loading surface; while at a moderate impact velocity, it appears as "V"-shaped bands ("V" mode) at the crushing edge. When crushing in the x_2 direction, two types of deformation modes ("V" mode and "I" mode) are found.

In our numerical simulations, at a low impact velocity, double-"V"-shaped bands located at the crushing edge and at the support edge are observed, as shown in Fig. 5a. This seems different from the "X"-shaped bands in Ref. [19], In fact, these two different configurations, "X"-shaped bands and double-"V"-shaped bands, are both Quasi-static crushing mode and caused by the weakest links in a fairly homogeneous stress field. The location of the static crushing bands, however, is highly sensitive to the details of boundary conditions and specimen height-to-width ratio. In the present case, the specimen height-to-width ratio of Model A is about 0.83, the same as that in Ref. [19]. But the boundary conditions adopted here differ from those in Ref. [19]. The specimens can slip on the rigid support plate with slight friction, while in Ref. [19], all degrees of freedom of the support edge of the specimen were fixed.

With the increase of the impact velocity, inertia effect becomes important and deformation trends to localization. The "V"-shaped bands at the support edge vanish and the "V"-shaped bands at the crushing edge occur closer to the edge, Fig. 5b. Finally, when the inertia effect is dominant, "I"-shaped bands are observed, as shown in Fig. 5c. They are similar to those of Ruan et al. [19].

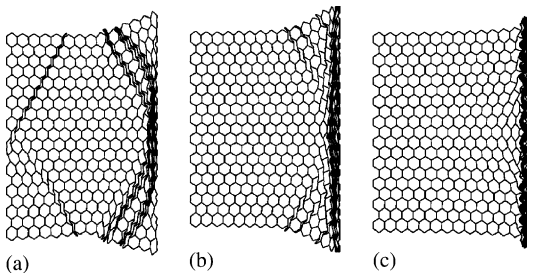

Fig. 5. Three patterns of a regular honeycomb crushed in the x_1 direction at different velocities of (a) $v = 5$ m/s, (b) $v = 20$ m/s and (c) $v = 80$ m/s with the displacement of $d = 36$ mm.

Considering the fundamental causes of each crushing configuration, the deformation modes can be catalogued into a Quasi-static mode (double "V" shape here or "X" shape in [19]), a Transitional mode ("V" shape), and a Dynamic mode ("I" shape).

3.1.2. Deformation modes of irregular honeycombs

Figs. 6–8 show deformation modes of a disordered honeycomb with $k_1 = 0.4$ crushed in the x_1 direction under various impact velocities. Under an impact velocity of $v = 5\,\mathrm{m/s}$, the specimen initially deforms with double-"V"-shaped bands, as shown in Figs. 6a and b. Increasing the displacement, multiple random shear bands appear, as shown in Fig. 6c. With further deformation, more random deformation bands develop progressively, Fig. 6d. The deformation exhibits a quasi-static nature that collapse occurs at the weakest links in a fairly homogeneous stress field. This result shows that the location of the quasi-static crushing bands is also highly sensitive to the cell irregularity, which leads to a complicated configuration and may help to improve the energy absorption capacity. Increasing the impact velocity, the inertia effect plays a more important role than the effect of the irregularity. For the case of $v = 20\,\mathrm{m/s}$ (Fig. 7), a Transitional mode takes place, where rare random shear bands and layerwise collapse bands appear and are localized near to the proximal surface. Increasing the impact velocity further (Fig. 8), a layerwise collapse mode with a narrow localized band is found, like that in the regular honeycomb shown in Fig. 5c.

In summary, it is found that the deformation of irregular honeycombs is more complicated than that of regular honeycombs but it can also be catalogued into a Quasi-static mode, a Transitional mode, and a Dynamic mode. Similar results are obtained for honeycombs with higher irregularity. Fig. 9 shows these modes of a disordered honeycomb with $k_1 = 0.8$ crushed in the x_1 direction under various impact velocities, while Fig. 10 shows those crushed in the x_2 direction. Fig. 11 shows these modes of a Voronoi honeycomb ($k_2 = 0.9$) crushed in the x_2 direction under various impact velocities.

3.1.3. Mode classification maps

According to the results of our numerical simulation, three mode classification maps are shown in Fig. 12 to identify the above deformation modes related with the impact velocity and the cell irregularity. The critical velocities at which deformation mode switches from one type to another are estimated. As shown in Fig. 12a, the deformation mode map for disordered honeycombs crushed in the x_1 direction is divided into three regions, i.e., the Quasi-static mode, the

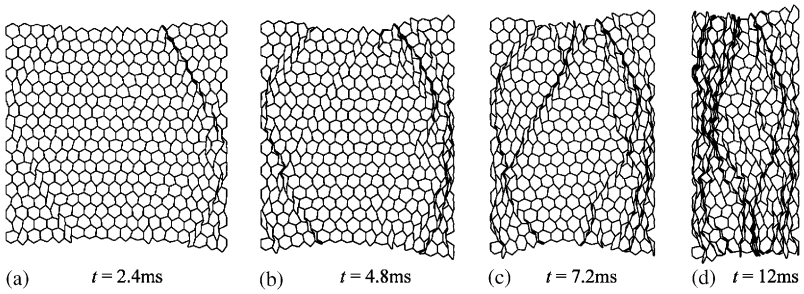

Fig. 6. Crushing of a disordered honeycomb ($k_1 = 0.4$) in the x_1 direction, $v = 5\,\mathrm{m/s}$.

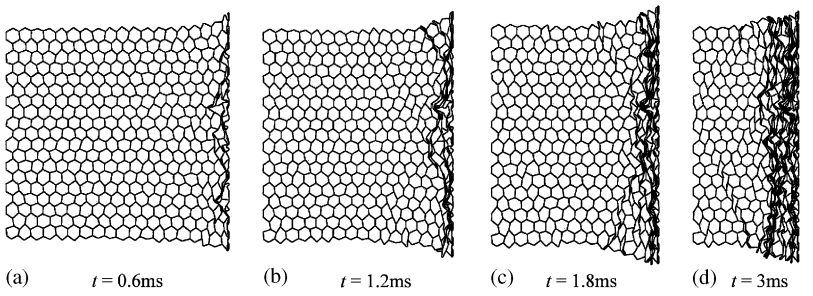

Fig. 7. Crushing of a disordered honeycomb ($k_1 = 0.4$) in the x_1 direction, $v = 20$ m/s.

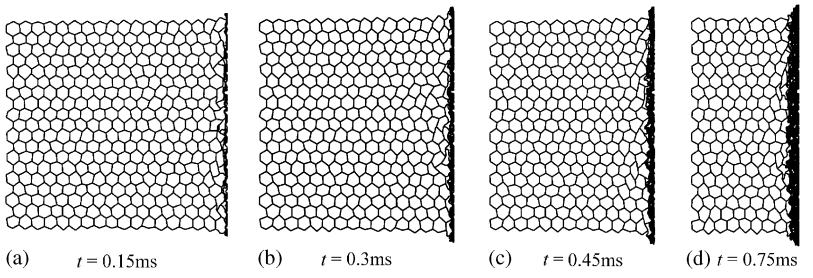

Fig. 8. Crushing of a disordered honeycomb ($k1 = 0.4$) in the x_1 direction, $v = 80$ m/s.

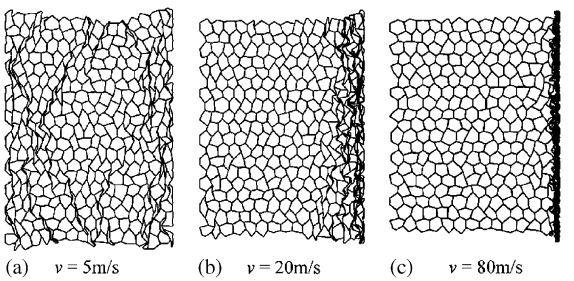

Fig. 9. Three patterns of a disordered honeycomb ($k_1 = 0.8$) crushed in the x_1 direction at different velocities with the displacement of $d = 36$ mm.

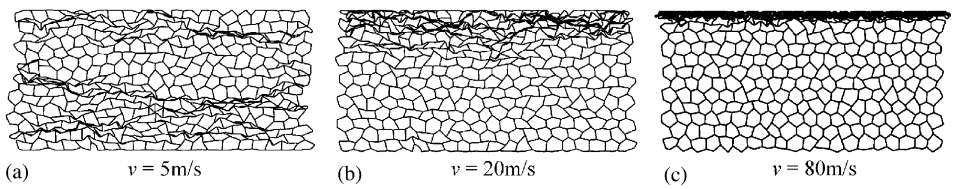

Fig. 10. Three patterns of a disordered honeycomb ($k_1 = 0.8$) crushed in the x_2 direction at different velocities with the displacement of $d = 36$ mm.

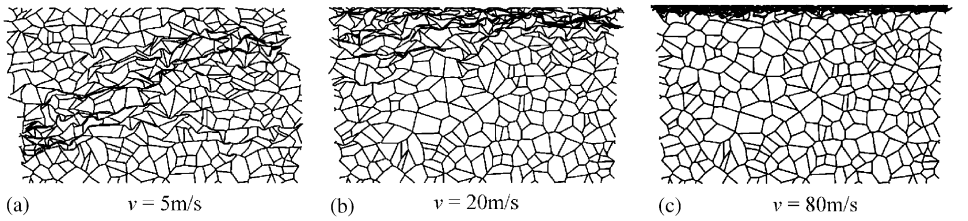

Fig. 11. Three patterns of a Voronoi honeycomb ($k_2 = 0.9$) crushed in the x_2 direction at different velocities with the displacement of $d = 36$ mm.

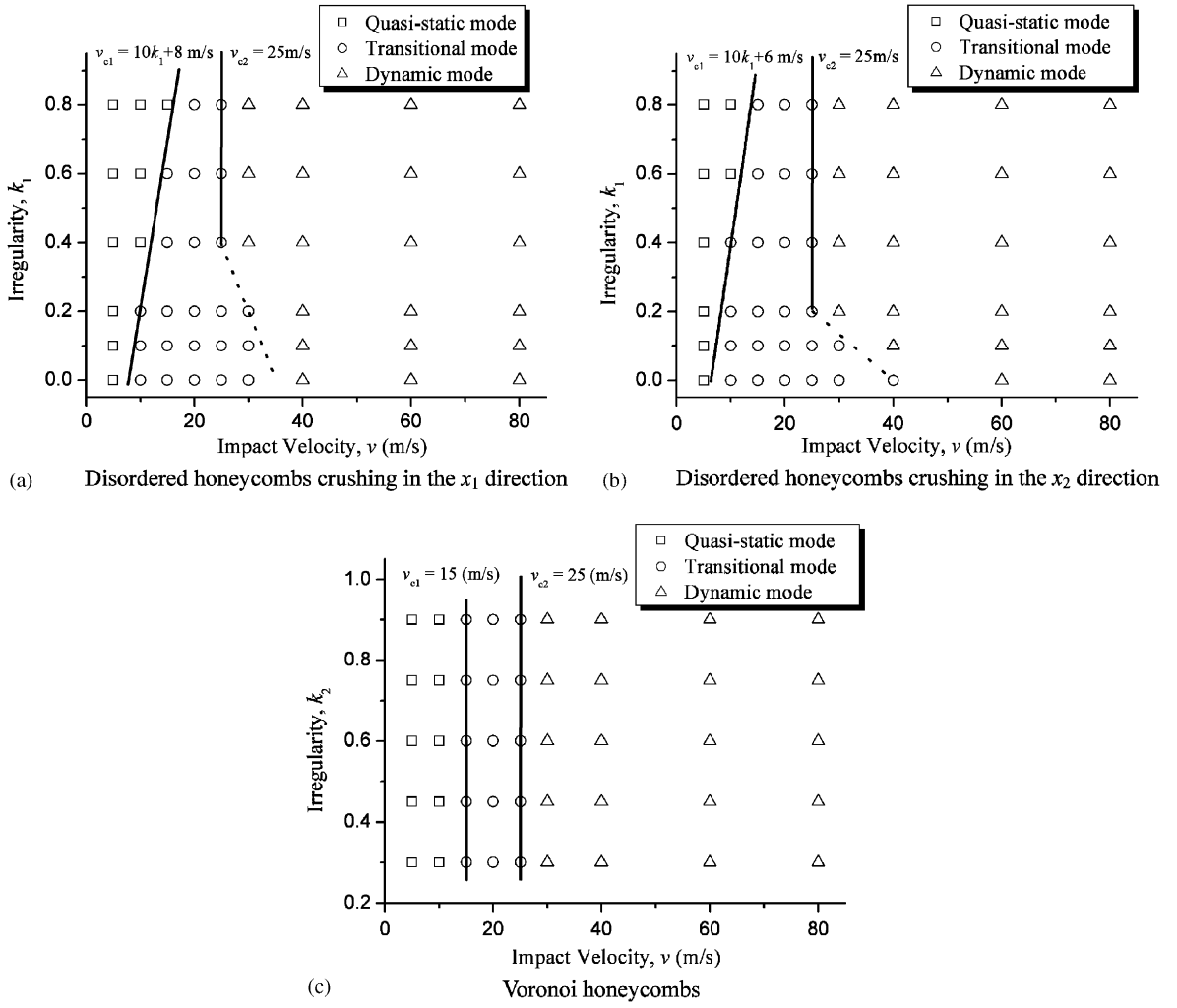

Fig. 12. Deformation mode maps for disordered honeycombs.

Transitional mode and the Dynamic mode, respectively, corresponding to various impact velocities and cell irregularities. Under a low impact velocity, honeycombs with a high irregularity are crushed in the Quasi-static mode with multiple random shear bands. Increasing the impact

velocity, this mode switches to a Transitional mode. The critical velocity can be estimated by an empirical equation that $v_{c1} = 10k_1 + 8(\mathrm{m/s})$, which implies that the critical velocity varies linearly with increasing irregularity. Increasing the impact velocity further, the Transitional mode develops into the Dynamic mode. For honeycombs with high irregularity ($k_1 > 0.3$), the critical velocity is almost constant, i.e., $v_{c2} = 25\,\mathrm{m/s}$, which is independent of the irregularity. However, for honeycombs with low irregularity ($k_1 < 0.3$), the critical velocity shows some dependence on the irregularity, i.e., the critical velocity increases with the regularity of the honeycombs. For disordered honeycombs crushed in the x_2 direction, it is similar with that crushed in the x_1 direction as shown in Fig. 12b. While for the Voronoi honeycombs, the critical velocities are almost constants, i.e., $v_{c1} = 15\,\mathrm{m/s}$ and $v_{c2} = 25\,\mathrm{m/s}$, respectively, as shown in Fig. 12c. It indicates that the Transitional mode may exist in a certain range of impact velocity despite the cell irregularity. In other words, the deformation characteristics mostly depend on the impact velocity.

3.2. Plateau crush pressures

The plateau crush pressure may depend on many parameters. In our simulation, we focus on the effects of the impact velocity and the cell irregularity. The plateau force is evaluated at the proximal surface with the striking distance from 10 to 60 mm. Fig. 13 shows the force–displacement curve and its corresponding plateau force for a disordered honeycomb of $k_1 = 0.4$ crushed in the x_1 direction at $v = 20\,\mathrm{m/s}$. The plateau crush pressures of regular honeycombs at various impact velocities are shown in Fig. 14. For each value of irregularity, 20 random samples for disordered honeycombs and 10 random samples for Voronoi honeycombs uniaxially crushed both in the x_1 direction and in x_2 direction are calculated.

3.2.1. Effect of the irregularity in transitional mode

The mean plateau crush pressure and its standard error for different value of irregularity (20 samples each) at $v = 20\,\mathrm{m/s}$ are calculated and shown in Fig. 15a. It transpires that the statistical plateau crush pressure slightly increases with an increase in the irregularity for disordered

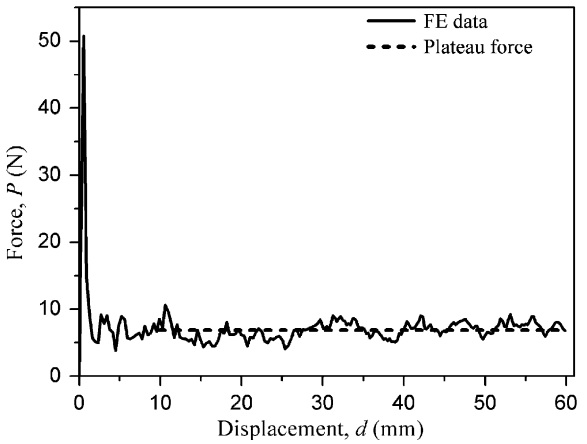

Fig. 13. Force–displacement curve and its plateau force for a sample calculated at the proximal surface.

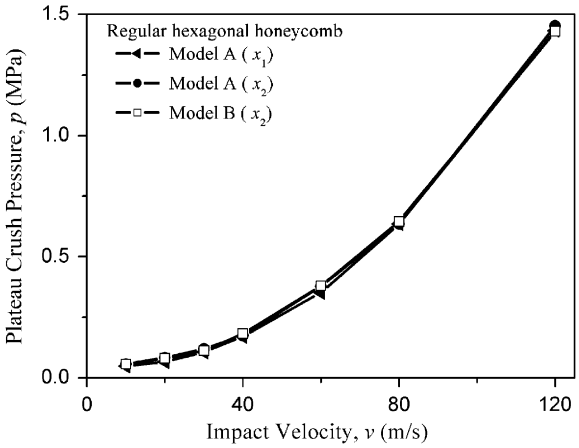

Fig. 14. The plateau crush pressures of regular honeycombs for in-plane dynamic crushing.

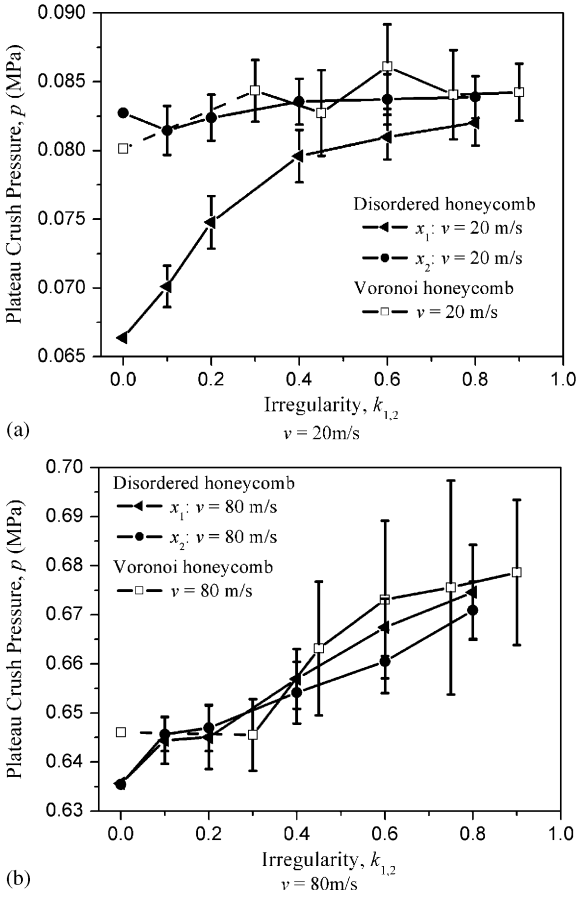

Fig. 15. Variation of plateau crush pressure with the irregularity.

honeycombs crushed in the x_2 direction, but it increases significantly with the increase in the irregularity for those crushed in the x_1 direction. Meanwhile, the plateau crush pressure of disordered honeycombs crushed in the x_2 direction is higher than that in the x_1 direction, which implies that the response of disordered honeycombs is anisotropic. In fact, a slight disorder of a regular honeycomb will not greatly change its morphology. With the increase of the irregularity, nevertheless, the deformation anisotropy vanishes, as shown in Fig. 15a.

The results of Voronoi honeycombs exhibit a stronger sensitivity to the sample randomicity. The second moment of the average number of edges per cell of Voronoi honeycombs shown in Fig. 4b is an important parameter, which characterizes the distribution of the number of edges per cell. A larger value of this parameter indicates a higher irregularity of the Voronoi honeycombs. Statistically, the mean plateau crush pressure has a slight variation with the irregularity of Voronoi honeycombs, similar as that of disordered honeycombs crushed in the x_2 direction.

3.2.2. *Effect of the irregularity in dynamic mode*

When the impact velocity is 80 m/s, irregular honeycombs are crushed in a Dynamic mode. The statistical plateau crush pressure is shown in Fig. 15b. The results show that the statistical plateau crush pressure increases with the increase in the irregularity. It reveals that at this impact velocity the relative energy absorption performance of cellular materials can be improved to a certain extent by increasing their irregularity.

3.2.3. *Effect of the impact velocity*

The statistical plateau crush pressures of disordered honeycombs with $k_1 = 0.4$ and Voronoi honeycombs with $k_2 = 0.6$ are calculated for different impact velocity, and compared to those of the regular honeycomb, as shown in Fig. 16. The results show that at an impact velocity near $v = 25$ m/s, the critical velocity of mode transition from the Transitional mode to the Dynamic mode, the increase in the relative energy absorption capacity by irregularity is obvious. The cause of this effect can be found from the deformation configuration. The number of deformation bands

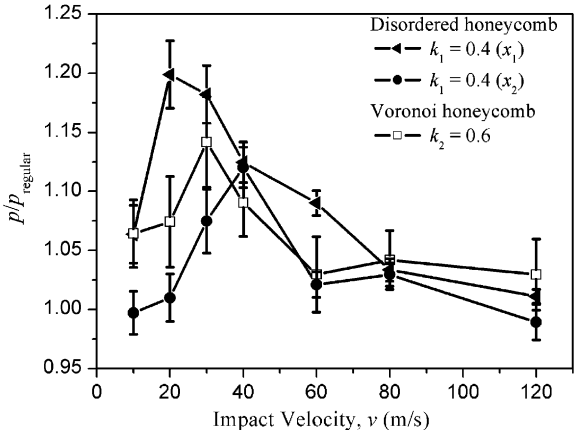

Fig. 16. Variation of relative plateau crush pressure with the impact velocity for irregular honeycombs.

in an irregular honeycomb is larger than that in a regular honeycomb. This effect is obvious especially at an impact velocity near the mode transition velocity v_{c2}. At a much high impact velocity, the inertia effect governs the response and the influence of irregularity vanishes.

4. Conclusions

Two types of irregular honeycombs are constructed to study the in-plane crushing behaviors. The influences of cell irregularity and impact velocity on the deformation mode and the plateau crush pressure are investigated by finite element method.

Three types of deformation modes are observed both in the regular honeycombs and in the irregular honeycombs. At a low impact velocity, the inertia effect is negligible and a Quasi-static mode, i.e., collapse of weak shear bands, takes place. At a high impact velocity, inertia effect dominates the deformation and a Dynamic mode, i.e., layerwise collapse of transverse band, occurs. A Transition mode with both localized shear bands and transverse bands exists for intermediate impact velocity. The numerical results show that the deformation configuration in an irregular honeycomb is more complicated than that in a regular honeycomb. For the irregular honeycombs at a low impact velocity, a Quasi-static mode appears with multiple random weak shear bands, in contrast with double-"V"-shaped bands found for the regular honeycombs. However, this difference vanishes at a much higher impact velocity while the inertia effect dominates the deformation. Mode classification maps of irregular honeycombs have been established considering the effect of the irregularity and the impact velocity, and the critical velocities for the irregular honeycomb under study were evaluated and expressed by empirical equations.

In our simulations, the statistical results show that the plateau crush pressure of an irregular honeycomb is higher than that of a regular honeycomb with the same density, mean cell size and material properties. The statistical plateau crush pressure increases with the increase in the cell irregularity. The relative increase is especially strong at an impact velocity near the mode transition velocity v_{c2}. It shows that at a moderate impact velocity the deformation complication is strongly caused by the irregularity of the 2D cellular structures, which improves the energy absorption performance.

The deformation mode, mode transitions and the plateau crush pressure may depend on many other factors such as the relative density, the cell size and the material properties. In this study, we focus only on the effects of the impact velocity and the cell irregularity. Other factors such as the relative density may affect the response and need to be investigated in further work.

Acknowledgements

This work is supported by the National Natural Science Foundation of China (project No. 10072059, No. 90205003 and No. 10302027) and the CAS K.C. Wong Post-doctoral Research Award Fund.

References

[1] Gibson LJ, Ashby MF. Cellular solids: structures and properties, 2nd ed. Cambridge: Cambridge University Press; 1997.
[2] Shi G, Tong P. The derivation of equivalent constitutive equations of honeycomb structures by a two scale method. Comput Mech 1995;15(5):395–407.
[3] Wang F, Li JR, Yu JL. A study of instability and collapse of aluminum honeycombs under uniaxial compression. Acta Mech Sinica 2001;33(6):741–8 (in Chinese).
[4] Papka SD, Kyriakides S. In-plane compressive response and crushing of honeycomb. J Mech Phys Solids 1994;42:1499–532.
[5] Papka SD, Kyriakides S. In-plane crushing of a polycarbonate honeycomb. Int J Solids Struct 1998;35(3–4):239–67.
[6] Papka SD, Kyriakides S. Experiments and full-scale numerical simulations of in-plane crushing of a honeycomb. Acta Mater 1998;46(8):2765–76.
[7] Papka SD, Kyriakides S. Biaxial crushing of honeycombs—Part I: Experiments. Int J Solids Struct 1999;36(29):4367–96.
[8] Papka SD, Kyriakides S. In-plane biaxial crushing of honeycombs—Part II: Analysis. Int J Solids Struct 1999;36(29):4397–423.
[9] Triantafyllidis N, Schraad MW. Onset of failure in aluminum honeycombs under general in-plane loading. J Mech Phys Solids 1998;46(6):1089–124.
[10] Fortes MA, Ashby MF. The effect of non-uniformity on the in-plane modulus of honeycombs. Acta Mater 1999;47(12):3469–73.
[11] Chen C, Lu TJ, Fleck NA. Effect of imperfections on the yielding of two dimensional foams. J Mech Phys Solids 1999;47(11):2235–72.
[12] Guo XE, Gibson LJ. Behavior of intact and damaged honeycombs: a finite element study. Int J Mech Sci 1999;41(1):85–105.
[13] Silva MJ, Hayes WC, Gibson LJ. The effects of non-periodic microstructure on the elastic properties of two-dimensional cellular solids. Int J Mech Sci 1995;37(11):1161–77.
[14] Zhu HX, Hobdell JR, Windle AH. Effects of cell irregularity on the elastic properties of 2D Voronoi honeycombs. J Mech Phys Solids 2001;49(4):857–70.
[15] Fazekas A, Dendievel R, Salvo L, Bréchet Y. Effect of microstructural topology upon the stiffness and strength of 2D cellular structures. Int J Mech Sci 2002;44(10):2047–66.
[16] Zhao H, Gray G. Crushing behavior of aluminium honeycombs under impact loading. Int J Impact Eng 1998;21(10):827–36.
[17] Hönig A, Stronge WJ. In-plane dynamic crushing of honeycomb. Part I: crush band initiation and wave trapping. Int J Mech Sci 2002;44(8):1665–96.
[18] Hönig A, Stronge WJ. In-plane dynamic crushing of honeycomb. Part II: application to impact. Int J Mech Sci 2002;44(8):1697–714.
[19] Ruan D, Lu G, Wang B, Yu TX. In-plane dynamic crushing of honeycombs—a finite element study. Int J Impact Eng 2003;28(2):161–82.
[20] Yu JL, Li JR, Hu SS. Strain-rate effect and micro-structural optimization of cellular metals. Mech Mater, accepted for publication.
[21] Hibbitt, Karlsson & Sorensen, Inc. ABAQUS/Explicit User's Manual, V6.3, 2002.
[22] Voronoi GM. Nouvelles applications des paramèters continus à la théorie des formes quadratiques. Deuxième Mémorie: Recherches sur les paralléloèdres Primitifs. J Reine Angew Math 1908;134:198–287.
[23] Zhu HX, Thorpe SM, Windle AH. The geometrical properties of irregular two-dimensional Voronoi tessellations. Philos Mag A 2001;81(12):2765–83.
[24] Schaffner G, Guo XDE, Silva MJ, Gibson LJ. Modelling fatigue damage accumulation in two-dimensional Voronoi honeycombs. Int J Mech Sci 2000;42(4):645–56.